

Dear referees,

Thank you for your comments concerning our manuscript entitled “*Characterization of liquid cloud profiles using global collocated active radar and passive polarimetric cloud measurements*” (ID: *egusphere-2025-2471*). Those comments are all valuable and very helpful for revising and improving our paper, as well as the important guiding significance to our researches. We have studied comments carefully and have made correction which we hope meet with approval. Revised portions are marked in blue (referee #1) /orange (referee #2) in our response document. The relevant references are at the end of our reply letter. The main corrections in the paper and the responses to the referees' comments are as following:

Response to Referee #1's Comments

General Summary

This paper presents an innovative methodology for characterizing vertical profiles of stratiform liquid clouds. The authors identify dominant morphological patterns of cloud effective radius profiles using CloudSat radar data, and then develop a way to retrieve profile information from passive polarimetric (POLDER) satellite observations. The paper is technically strong and well written. However, after reading the paper I was left with a few key questions that should be addressed before publication

Major Comment 1: The authors state that cloud-base height is retrieved “based on POLDER data” (line 116). How, exactly, is this retrieval performed? I was not aware that cloud base height could be retrieved from POLDER. Does the multivariate regression model mentioned in line 367 also use cloud base height from POLDER?

Response: Thank you for your question. Obtaining cloud bottom heights based on POLDER data is another work in progress by the authors associated with this paper, which has been completed but not formally published, and is currently being submitted to relevant academic journals for review, so we do not describe this work in detail in this manuscript, and the multivariate linear regression model mentioned in line 367 in this study also uses the cloud bottom heights inverted by this method as input. We describe here the implementation of the method to obtain cloud bottom heights based on POLDER data to answer the questions raised by the referee:

We developed a machine learning-based approach to estimate cloud base height (CBH) from POLDER/Parasol observations by leveraging collocated CloudSat radar measurements. The dataset was constructed by matching Parasol Level 1 (L1) data—including oxygen absorption (OA) channels (763 nm and 765 nm), OA ratios across 14 viewing angles, longitude, latitude, and elevation—with CloudSat Level 2 (L2) CBH products for March, June, September, and December 2007. Spatial collocation accuracy was constrained to within 0.01°, while temporal discrepancies were negligible due to the near-simultaneous observations from A-Train satellites. To ensure high-quality training data, only cases where Parasol confidently detected cloudy scenes and CloudSat identified single-layer clouds were retained. The dataset was split into training and validation subsets, with 7 days per month reserved for independent evaluation. The machine learning model used geographic coordinates (longitude, latitude, elevation) and

Parasol’s multi-angle OA information as inputs to predict CBH, with CloudSat-derived heights serving as ground truth. After optimization and validation, the finalized model enabled global CBH retrieval using Parasol L1 data alone, providing a novel solution for passive sensor-based cloud vertical structure characterization. This method addresses the inherent limitations of passive remote sensing in directly probing cloud boundaries while capitalizing on POLDER’s unique multi-angle OA capabilities. After several machine learning algorithms are compared, the deep neural network (DNN) model with the best accuracy is selected as the retrieval model. The method of CBH reversal based on multiangle OA remote sensing and the DNN has a mean absolute error (MAE) of 0.78 km, a bias of 0.22 km, and a correlation coefficient (R) of 0.82. By integrating machine learning with the multiangle OA, this method offers a novel approach for CBH retrieval. Fig. R1 shows the specific process of our CBH retrieval algorithm.

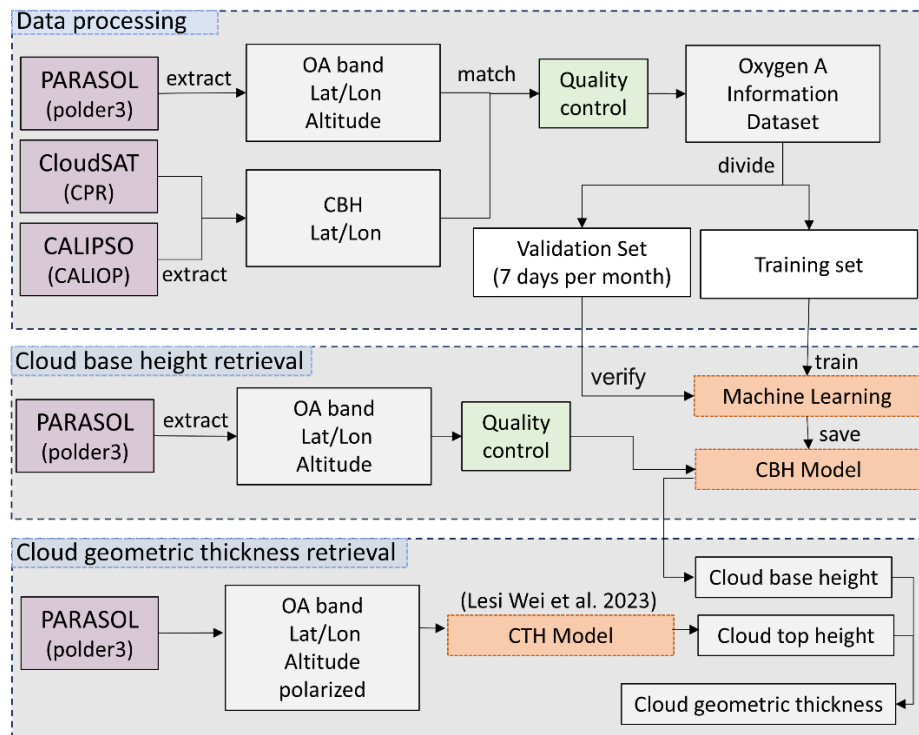


Figure R1. Flowchart of the machine learning-based algorithm for retrieving CBHs using the OA (Ji et al. 2025. Manuscript submitted for publication)

Detailed modifications are as follows: We have added the explanation to Line 118-119: “[The retrieval algorithm for cloud base height will be thoroughly described in a forthcoming article and is therefore not discussed here.](#)”

Major Comment 2: The spatial resolution of CWC-RO (less than 2km) is vastly different from the spatial resolution of POLDER (~50km). I'd like to see more details about how the observations were matched up in creating Figure 9, and more discussion about whether relationships between variables derived at CloudSat resolution should be expected to hold at POLDER resolution, when there will be a lot of sub-pixel heterogeneity.

Response: Thank you very much for your suggestions. The issues you raised are crucial and will be essential for us to enhance the completeness of the paper and demonstrate the robustness of the estimated method for cloud-top profile structural characteristics.

(1) First, addressing your initial question: The purpose of the experiment in Fig. 9 is to estimate the profile turning point CER (TP_CER) and normalized optical thickness (TP_NCOT) using passive data, and to compare these results with active data. This aims to explore the feasibility of the aforementioned method for estimating profile characteristics in passive data. The matching process is as follows: We began by identifying matching pairs of POLDER3 and CloudSat data from March 2007, focusing on orbits that contained both datasets and included a high number of stratiform cloud profiles with a triangular shape. From these, we selected the POLDER3 data recorded between 06:41:09 and 07:24:06 on March 2, 2007, along with the corresponding CloudSat data, to estimate and validate the profile TP parameters.

We primarily used POLDER Level 2 data (RB2) for matching with CloudSat. The spatial resolution of POLDER RB2 product is approximately 16 km, which differs from CloudSat's spatial resolution (less than 2 km). Therefore, during the matching process, we calculated the Euclidean distance between each POLDER_RB2 pixel and the corresponding CloudSat data point. Due to the coarser resolution of POLDER_RB2 data compared to CloudSat, multiple CloudSat data points may correspond to the same POLDER_RB2 pixel. We retained only the CloudSat data point closest to the center of the POLDER_RB2 pixel. Ultimately, eight cases were randomly selected (Fig. 9) for validating the estimated characteristics of the profile structures.

Through matching, we extracted COT, latitude, longitude and other related data from the POLDER_RB2 product. Using these coordinates, we further extracted CBH, CTH, and CT_CER data retrieved by our algorithm. CBH and CTH were retrieved from POLDER3 Level 1 products with a resolution of 6 km, matching the L1 product resolution. CT_CER was also retrieved from POLDER L1 product with a 50 km resolution. POLDER lacks near-infrared bands, so it can only retrieve cloud-top CER using multi-angle polarization signals. This method has a drawback: it must compensate for insufficient angular sampling by including more pixels—resulting in lower resolution for the retrieved CER. Our current algorithm (Shang et al., 2019) can achieve CER retrieval at a range of 40 – 60 km. This paper utilizes the retrieved 50 km resolution CER product. However, we do not consider this an insurmountable permanent flaw. Internationally, there are currently polarimetric multi-angle payloads with higher spatial resolution and greater observation angles that have been launched or are planned for launch. For instance, China's DPC/GF-5 achieves a spatial resolution of nadir 3.3 km; the 3MI/Metop-SG developed by the European Space Agency offers a spatial resolution of nadir 4 km, supports up to 21 observation angles, and incorporates near-infrared bands. These capabilities collectively enable higher-resolution CER retrieval.

(2) We understand your concerns regarding sub-pixel heterogeneity due to the coarse resolution of POLDER data, as well as the challenges in applying relationships derived from CloudSat to POLDER data because of differing spatial resolutions. Our primary response is as follows: (a)

Our primary research subject is single-layer stratiform liquid clouds (stratocumulus and stratus). Relevant literature indicates (Jr., 2014) that within stratiform cloud regions, both updrafts and downdrafts are relatively weak. They are relatively uniform horizontally compared to other cloud types, and their cloud microphysical properties exhibit slow horizontal variations—that is, they are less spatially heterogeneous. This is why we selected single-layer stratiform liquid clouds—a structurally simpler cloud type—as our primary research subject. (b) Shang et al. (2015) specifically investigated the impact of liquid cloud spatial heterogeneity on CER retrieved from POLDER. The Table 2(Fig. R2) presented in their paper shows that under sub-grid scale heterogeneity, the relative deviation between the retrieved CER and the sub-grid scale CER mean ranges from 0.86% to 8.33% (Table R1), with none exceeding 10%. This indicates that for liquid clouds, the impact of sub-grid scale heterogeneity on the retrieval of a representative CER value is manageable and typically within an acceptable range (under 10%) for bulk microphysical properties.

Table 2. Retrievals from a heterogeneous cloud field with variable CDRs using POLDER-like polarized reflectances (865 nm) in 137–165° and 145–165° ranges, respectively. In all cases, the EV in the sub-scale cloud and the COT were assumed to be 0.01 and 5, respectively. The “+” indicates the equal share of the CDRs in the cloud fields. The mean CDR and EV indicate the effective radii and variances for the combined droplet size distributions. The CDR and EV estimates are restricted with $T_1 > 0.978$ and $T_2 < 0.01$.

Combined CDRs (μm)	Sub-scale EV	Mean CDR (μm)	Mean EV	Retrievals of 137–165°		Retrievals of 145–165°	
				CDR (μm)	EV	CDR (μm)	EV
5 + 10	0.01	9.00	0.06	–	–	–	–
5 + 15	0.01	14.00	0.06	–	–	–	–
5 + 20	0.01	19.12	0.04	–	–	–	–
10 + 15	0.01	13.46	0.04	13.0	0.1	–	–
10 + 20	0.01	18.00	0.06	16.5	0.1	–	–
15 + 20	0.01	18.20	0.03	17.5	0.05	10.0	0.02
5 + 10 + 15	0.01	12.70	0.11	12.0	0.1	–	–
5 + 10 + 20	0.01	16.92	0.13	–	–	–	–
5 + 15 + 20	0.01	17.35	0.08	17.5	0.05	–	–
10 + 15 + 20	0.01	17.07	0.06	16.0	0.1	16.5	0.01

Figure R2. Table 2 from Shang et al. (2015), AMT.

Table R1. Relative deviation between inverted CER and subpixel CER mean values.

	Mean CER(μm)	Retrieval CER(μm)	Relative deviation
1	13.46	13	-3.41%
2	18.00	16.5	-8.33%
3	18.20	17.5	-3.85%
4	12.70	12.0	-5.51%
5	17.35	17.5	+0.86%
6	17.07	16.0	-6.27%

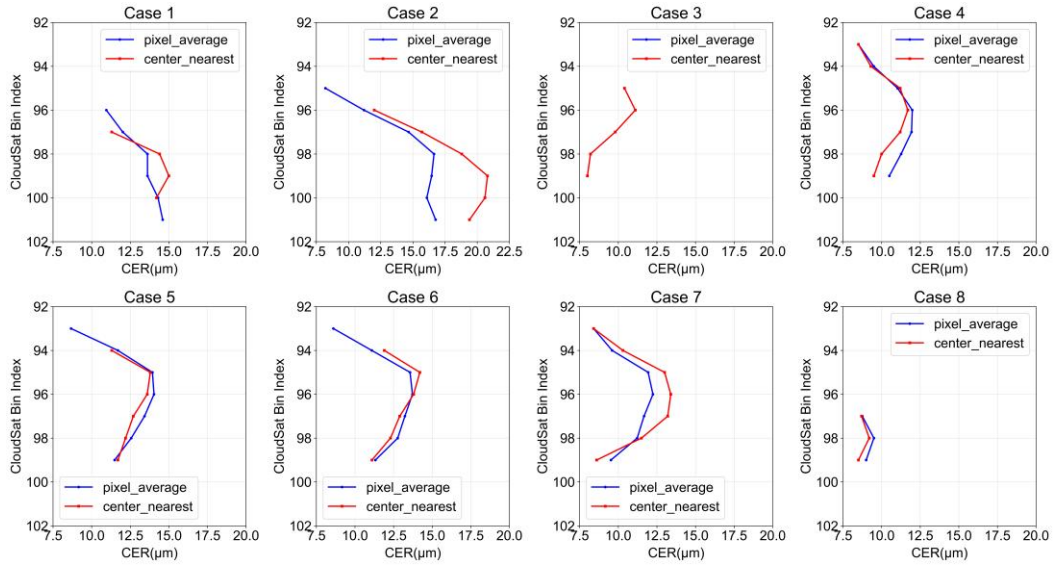


Figure R3. Comparison of the average CER profile (averaged by height) within the same POLDER pixel versus the CER profile closest to the center of the POLDER pixel.

(c) To further investigate whether the relationship derived from CloudSat could be applied to POLDER data, we statistically analyzed the CloudSat CER profiles corresponding to these 8 POLDER pixels. For each POLDER pixel, we averaged the CloudSat CER profiles and compared them with the CloudSat profile closest to the center of the POLDER pixel. The results are shown in Fig. R3. We conclude that, except for a slightly higher deviation in Case 2, the deviations in other cases are relative small. That is, the profiles at the coarse resolution of the POLDER level (pixel_average) show little difference from the CloudSat profiles at normal resolution that we selected (center_nearest), demonstrating a high degree of similarity.

In summary, we believe that although single-layer stratiform liquid clouds exhibit spatial heterogeneity, this heterogeneity is relatively weak. This allows the relationships derived at CloudSat resolution to be applied to coarser-resolution POLDER data. However, we acknowledge that this spatial averaging inherent to coarse resolution data is the primary challenge when inferring detailed vertical profile features, as discussed in our response to the other referee's similar concern. In the future, as the observational capabilities of passive multi-angle polarization payloads improve, the association between active and passive observation data will become even stronger.

Detailed modifications are as follows: We have added the description of match-up process in Section 3.4. “To validate the profile structural characteristics retrieved by passive satellite observations, a match-up process between POLDER and CloudSat observations is conducted. We focus on March 2007 and identified coincident orbits that contained a high number of stratiform cloud profiles exhibiting a triangle-shaped vertical structure in CloudSat data. A specific dataset from March 2, 2007 (POLDER observation time between 06:41:09 and 07:24:06 UTC) is selected for detailed analysis in Section 4.4. The POLDER-3 Level 2 (RB2) product served as the primary dataset for matching with CloudSat observations. With a spatial resolution of approximately 16 km, this product is notably coarser than CloudSat's resolution

of less than 2 km. To establish correspondence between the datasets, the Euclidean distance between each POLDER-3 RB2 pixel center and all CloudSat data points within the POLDER-3 RB2 pixel is computed. Owing to the resolution discrepancy, a single POLDER-3 RB2 pixel often contains multiple CloudSat data points. In such cases, only the CloudSat data point closest to the center of the POLDER_RB2 pixel is retained.

Through the matching process, cloud optical thickness (COT), latitude, longitude, and other relevant data are extracted from the POLDER-3 RB2 product. These coordinates are then used to extract cloud base height (CBH), cloud top height (CTH), and cloud-top effective radius (CT_CER) obtained through the retrieval algorithm. CBH and CTH are retrieved from the POLDER-3 L1 product, which has a native resolution of 6 km, matching the resolution of the source data. CT_CER is retrieved from the POLDER L1 product at a 50 km resolution.”

Meanwhile, we have added a discussion regarding the uncertainties arising from the coarse resolution of POLDER in Section 5. “The coarse resolution of POLDER products restricts the ability to capture sub-pixel cloud heterogeneity; however, by concentrating on relatively uniform single-layer stratiform liquid clouds, this study partially mitigates the resulting retrieval uncertainties. It should be noted that sub-pixel heterogeneity can inevitably introduce certain errors, particularly at cloud boundaries. Nevertheless, Shang et al. (2015) pointed out that the error caused by sub-pixel heterogeneity in cloud effective radius (CER) retrieval does not exceed 10%, which remains within an acceptable range.”

Minor Comment 1: Line 136: Why 2013, 2019, and the first eight months of 2020? This seems like a very arbitrary group of years to use.

Response: The choice of data from 2013, 2019, and the first eight months of 2020 for this study was carefully considered. Our aim was to explore cloud profile structures by combining CloudSat observations with polarized multi-angle payload data. In our preliminary work, we gathered available polarized multi-angle measurements from sources such as the French POLDER-3/PARASOL instrument, as well as China's DPC/GF-5 and DPC/GF-5(02) sensors. Based on our initial assessments, CloudSat's key CWC_RO product provides reliable data between 2006 and August 2020, while POLDER-3's useful dataset covers 2005 to 2013. Additionally, we had access to China's DPC/GF-5 and DPC/GF-5(02) data, though it should be noted that these datasets are not publicly available. However, the DPC data at our disposal is limited to 2019 and 2020. To ensure our analysis remains as up-to-date as possible while still allowing for joint active-passive sensor studies, we ultimately selected CloudSat data from 2013, 2019, and the first eight months of 2020 for this investigation.

Minor Comment 2: Line 204: As far as I am aware, there is no “Colorado State University regional climate model.” Do you mean the CSU Regional Atmospheric Modeling System (RAMS)?

Response: Thank you for your reminding, we feel sorry for our carelessness. In our

resubmitted manuscript, we have corrected the “Colorado State University regional climate model” to “the Colorado State University Regional Atmospheric Modeling System (RAMS)”.

Minor Comment 3: It should be noted that the CloudSat CWC-RO product misses many (perhaps the majority of) single-layer liquid clouds, either because the clouds are masked by surface clutter or because they are below the radar's noise threshold (e.g., Lamar et al., 2020; Schulte et al., 2023). So the true nonprecipitating-to-precipitating ratio is likely much higher.

Response: We agree with this valuable comment. we have read the relevant papers carefully, CloudSat's data may indeed have this problem, so we try to expand the data scope to increase the amount of research data (single-layer liquid cloud). The ratio of non-precipitating clouds to precipitating clouds here is just a statistic of the data situation of our existing study, as you said, it may be different from the real ratio of non-precipitating clouds to precipitating clouds, the real ratio of non-precipitating clouds to precipitating clouds may be much higher, and we added this point to the article, as well as the possible uncertainty of CloudSat in the detection of single-layer liquid clouds.

Minor Comment 4: Line 240: I believe you mean Table A4 here, but even so, I do not understand what the table is intended to show.

Response: Yes, this refers to Table A4, which exists in order to explain the complex situation “Other” such profiles, there is also a part of the profile that is highly similar to the two main shapes derived from this study, and exists in order to make the shape analysis of the profiles more complete. It should be recognized that our interpretation of Table A4 is not complete, and we have added explanations in the note of Table A4: *situation1 refers to a situation where only one segment of the profile does not correspond to the increasing and then decreasing shape profile of shape1, and situation2 refers to a situation where only one segment of the profile does not correspond to the monotonically decreasing shape profile of shape2. There is an intersection of situation1 and situation2, i.e., a profile that matches both situation1 and situation2 (Intersection of 1+2), which needs to be subtracted out when calculating the sum of the two in order to avoid double counting.*

Minor Comment 5: Line 327: Any idea whether these two density centers have physical meaning?

Response: Thank you for raising this insightful question. From the Fig. 6(m), (n), and (p) of the original manuscript, i.e., the following Fig. R4(a1), (b1), and (c1), it can be observed that the scatter density distribution of the turning point CER(TP_CER) and the turning point LWC (TP_LWC) exhibits two density centers. This indicates that the relationship between TP_LWC and TP_CER is not a simple linear correlation. We conducted further analysis on the density centers, taking Fig. R4(a1) (sea non-precipitation clouds) as an example: the TP_CER shows a unimodal distribution clustered around 11–13 μ m, while TP_LWC exhibits a bimodal

distribution within the same TP_CER range of 11–13 μm . In other words, at the same TP_CER, some profiles have relatively higher TP_LWC, while others have relatively lower TP_LWC.

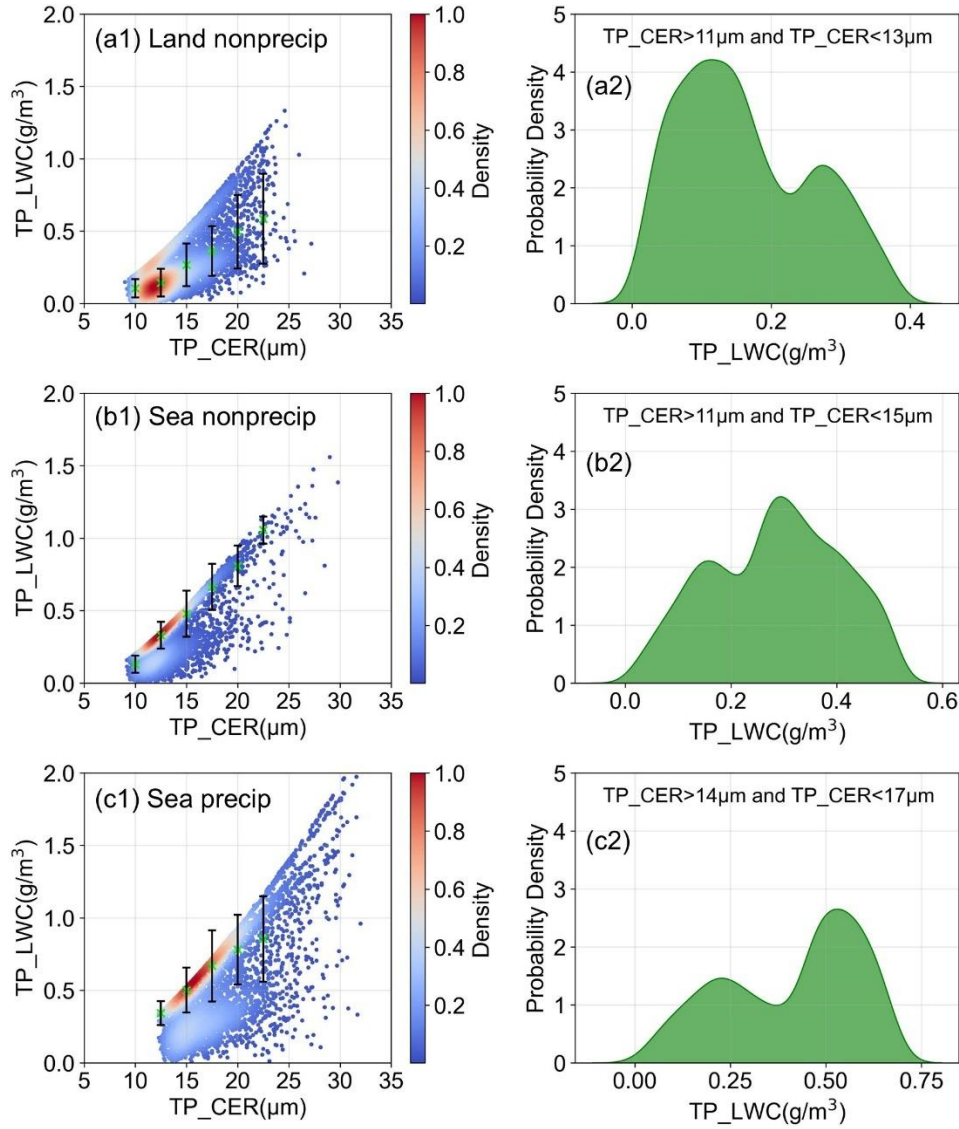


Figure R4. Scatter density plots exhibiting dual density centers and their corresponding probability density distribution of TP_LWC within a specific TP_CER range.

We propose that the two density centers reflect two dominant mechanisms governing cloud microphysical processes. One mechanism is primarily dominated by condensational growth, characterized by higher liquid water content for a given cloud droplet size. This typically occurs under conditions of low cloud condensation nucleus (CCN) concentration and a stable environment, where cloud droplets grow slowly through vapor condensation and accumulate liquid water. The other mechanism is dominated by collision-coalescence growth, exhibiting lower liquid water content for the same cloud droplet size. This often happens in environments with high CCN concentrations and dynamic activity, where cloud droplets grow rapidly through collision and coalescence, leading to the redistribution of liquid water into a fewer number of larger droplets. This conclusion is strongly supported by the observed land-sea

contrast: for sea-based clouds, the density center with higher liquid water content (as seen in Figures R4(b1) and (c1)) shows a higher concentration of data points, while for continental clouds, the density center with lower liquid water content (Figure R4(a1)) is more densely populated. Over the sea, the condensation-dominated mechanism—characterized by high liquid water content—is more prevalent, consistent with the typically low aerosol concentrations, abundant moisture supply, and stable thermodynamic conditions in marine environments. In contrast, over land, the collision-coalescence-dominated mechanism—associated with lower liquid water content—prevails, aligning with the high aerosol concentrations, strong convective activity, and dynamically active nature of continental settings. This systematic geographical pattern strongly affirms the physical reality of the dual density centers, demonstrating that they represent distinct cloud microphysical states driven by environmental factors such as aerosol concentration and thermodynamic conditions.

Detailed modifications are as follows: We have briefly expanded on the potential physical implications of the dual density centers in the original manuscript. “The two density centers observed in the relationship between the TP_CER and TP_LWC reflect two distinct cloud microphysical regimes. One is primarily driven by condensational growth, which tends to occur under low aerosol and stable conditions, resulting in higher LWC for a given droplet size. The other is dominated by collision-coalescence, typical in relative high aerosol and dynamically active environments, leading to lower LWC for the same droplet size.”

References:

- Jr., R. A. H.: Cloud Dynamics, 2nd, Academic Press 2014.
- Shang, H., Chen, L., Bréon, F. M., Letu, H., Li, S., Wang, Z., and Su, L.: Impact of cloud horizontal inhomogeneity and directional sampling on the retrieval of cloud droplet size by the POLDER instrument, Atmos. Meas. Tech., 8, 4931-4945, 10.5194/amt-8-4931-2015, 2015.
- Shang, H., Letu, H., Bréon, F.-M., Riedi, J., Ma, R., Wang, Z., Nakajima, T. Y., Wang, Z., and Chen, L.: An improved algorithm of cloud droplet size distribution from POLDER polarized measurements, Remote Sensing of Environment, 228, 61-74, <https://doi.org/10.1016/j.rse.2019.04.013>, 2019.